A novel cyclic thermal treatment for enhanced globularisation kinetics in Ti-6Al-4V alloy: experimental, constitutive and FE based analyses

Paul M. Souza*, Giribaskar Sivaswamy, Aurik Andreu, Salaheddin Rahimi

Advanced Forming Research Centre,
University of Strathclyde, 85 Inchinnan Drive, Inchinnan, Renfrew, PA4 9LJ, UK

paul.souza@strath.ac.uk; giribaskar.sivaswamy@strath.ac.uk; aurik.andreu@strath.ac.uk; salah.rahimi@strath.ac.uk

Abstract

Secondary hot-working on dual phase titanium alloys are essential for microstructural modification to tailor mechanical properties, which is typically challenging due to a narrow available processing window, especially during industrial scale manufacturing. Poor workability, strain induced porosity and adiabatic temperature rise in α/β phase region (i.e., sub-transus) are some of the main challenges faced. Cyclic thermal treatment (CTT) is an emerging technology showing potentials for microstructure modification (i.e., globularisation) in Ti-6Al-4V with significantly reduced mechanical work in the α+β region. This study summarises the results of CTT investigations conducted on a wrought Ti-6Al-4V alloy subjected to various thermo-mechanical conditions to develop different initial microstructures. Samples with uniform strain distributions were extracted from pre-forged samples and subsequently subjected to CTT using both conventional electric furnace (i.e., for slow heating and cooling rates), and induction heating (i.e., for faster heating and cooling rates). CTT of the samples forged at sub-transus temperature in conventional furnace led to maximum (i.e. ~ 100%) globularisation and significant coarsening of α grains, resulting in an equiaxed bimodal microstructure. On the other hand, CTT with induction heating method has resulted in a maximum of 80% globularisation fraction in samples forged to 60% reduction, and ~ 35% globularisation fraction in those forged to 20% reduction. The globularisation mechanisms during CTT of the sub-transus forged samples was dominated by the boundary splitting and thermal grooving. A Johnson-Mehl-Avarmi-Kolmogorov (JMAK) based model has been developed to predict the evolution of globularisation and grain growth during CTT. The developed JMAK model was then successfully incorporated into DEFORM® software as post-processing user subroutines. The predicted microstructure evolution by Finite Element (FE) simulations shown a good convergence towards the experimentally measured data following CTT.

Keywords: Metals and alloys; microstructure; phase transitions; computer simulations; scanning electron microscopy, SEM

1.0 Introduction

Dual phase titanium alloys play a major role in the aerospace sector due to their high strength to weight ratio, strength to toughness ratio and superior corrosion resistance. One of the mainly used and studied material within this class of alloys is Ti-6Al-4V, which is predominantly used as a wrought product in the aerospace sector compared to as-cast condition in the marine sector [1] . Thermo-mechanical processing are necessary to control microstructural characteristics in Ti-6Al-4V to tailor its final mechanical properties. The secondary α/β processing, typically within a narrow range of temperatures below β transus and industrially viable strain rates, is adopted for microstructural modification known as the globularisation, which requires meticulous process control. This is due to the high possibility of variation in α and β phase fractions and their morphologies, potentially leading to inferior mechanical properties [2, 3]. Secondary processing increases manufacturing costs of components, especially those used for structural applications. For instance, secondary processing required to obtain a 25 mm thick plate leads to 47% increase in the overall manufacturing cost [4]. Hence the possibilities of adopting alternate manufacturing routes are explored by manufacturers.

A number of alternative manufacturing routes have been reported for titanium extraction from the ore [5] and manufacturing through powder metallurgy route [4]. The additive manufacturing, powder metallurgy and cost effective hybrid processing routes like field-assisted sintering technique (FAST) [4] are some of the important alternative methods developed for manufacturing parts with complex geometries, with varied chemical compositions, minimised material wastage and cost reduction [6]. However, these processes are limited in terms of the production volume and most importantly microstructure characteristics of the finished product. The challenge is to obtain a microstructure with suitably modified grain morphology (i.e., equiaxed) to produce components with higher strength and toughness. There are studies attempting to understand the effect of various heat treatments on the evolution of microstructure without changing the shape and dimensions of the billets (i.e., with minimal deformation) that were based on multi-step annealing at high temperatures [6-8].

Cyclic Thermal Treatment (CTT) process has recently found a significant interest among researchers for its potential to design and control microstructural morphology in titanium alloys. CTT involves heating and cooling cycles within a stipulated temperature range under a specified heating/cooling rate [9]. Previous studies have reported significant alterations in the fraction of subgrain boundaries in Ti-6Al-4V alloy with varying initial microstructures subjected to CTT under

different process parameters [9]. A recent report on Ti-6Al-4V alloy, produced through additive manufacturing, showed that 24 hours CTT had resulted in an equiaxed bimodal microstructure [6]. However, the potential of CTT to globularise the martensitic/Widmannstatten microstructure during wrought processing has not been addressed and requires further research. This could substantially reduce the secondary processing cost of titanium alloys. Moreover, cost effective process route to tailor the microstructure of Ti-6Al-4V alloy with minimised heterogeneity can increase the reliability of the wrought components for numerous applications.

The present work is focused on the development and understanding of the CTT by conducting systematic experimental trials on Ti-6Al-4V alloy to generate sufficient data on its effect on microstructural modifications. To explore the suitability of the CTT for faster industrial processing, the efficacy of both furnace heating and induction heating are studied with varying heating and cooling rates. Additionally, finite element (FE) modelling of the process, considering the pre-CTT strain and prior mechanical working history has also been developed. Empirical material models, relating the grain refinement and globularisation of α phase to the CTT process, are incorporated into the FE simulation as a user routine to predict the evolution of microstructure, and the results are compared with the results of experimental trials.

2.0 Experimental methodologies

2.1 Material

A forged billet of Ti-6Al-4V alloy supplied by TIMET, with 85 mm diameter and nominal chemical compositions of 6.4% Al, 4.0% V, 0.15% Fe, 0.017% C, 0.18% O, 0.005% N (wt%) was used for these investigations. The β transus temperature of a same grade of alloy with similar chemical compositions was reported to be in the range of ~ 995±5 °C [10]. Cylindrical samples with 85 mm diameter (i.e., same as the initial billet) and 85 mm height were cut from the as-received billet using a band saw, and subsequently subjected to β solution treatment at 1020 °C for 2 hours followed by water quenching to room temperature (Fig. 1a). The samples were coated with delta glaze to minimise oxidation and α-case formation during heat treatments.

2.2 Forging

The β solution treated samples were then subjected to uniaxial hot open-die forging at two different temperatures including 950 °C and 1050 °C. These were to understand the effects of hot-working at both α+β and β phase region on microstructure evolution during the subsequent cyclic heat treatments. Three samples were forged to different levels of reduction in height (i.e., 20%, 40% and 60%) at 950 °C and a sample was forged similarly to 60% reduction at 1050 °C in one step. For

all cases, the sample was soaked at the target temperature for 90 minutes to obtain a uniform temperature distribution prior to forging.

The forging experiments were carried out using a 500 T hydraulic press fitted with self-heated flat dies. Both the top and bottom dies were pre-heated to ~ 400 °C. The dies were sprayed with a water-based graphite lubricant immediately before forging to minimise friction with the sample during forging. The heated samples were transferred from the furnace quickly to the bottom die to minimise temperature loss. For all experiments, the average ram velocity was ~ 6 mm/s, thus providing a true axial strain rate during forging (= ram velocity/instantaneous height) in the range between ~ 0.05 and 0.5 s^{-1}. The samples were water quenched to room temperature within 10 seconds after forging (Fig. 1a).
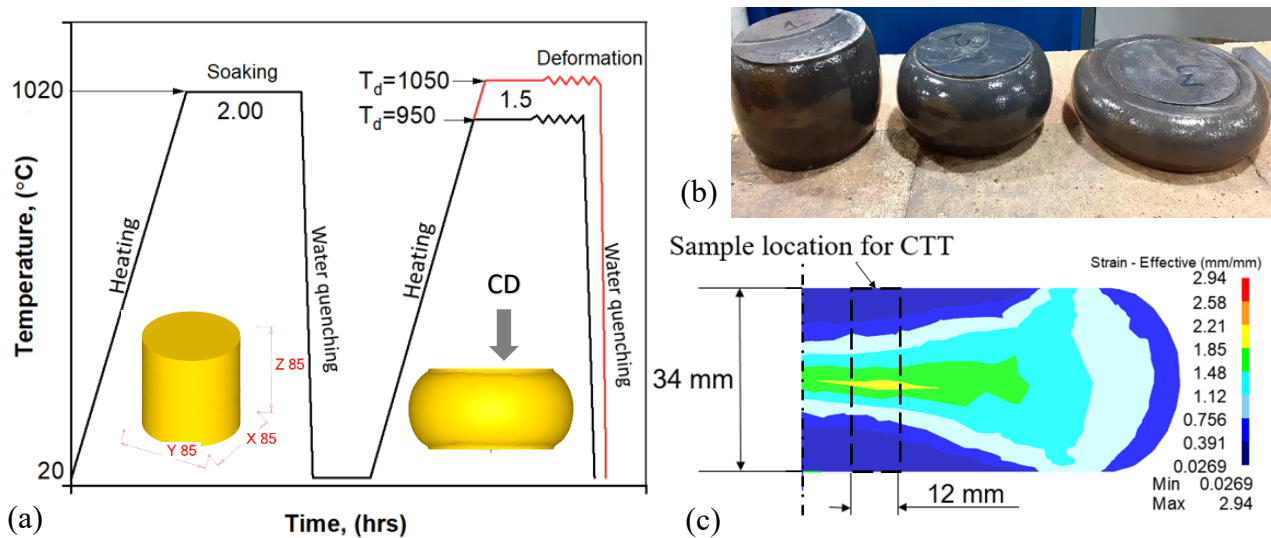

Figure 1: (a) Schematic representation of β solution heat treatment and subsequent open die forging carried out at both α+β range and full β phase region. T_d is the deformation temperature, (b) A photograph of the samples forged at 950 °C (i.e., α+β range) to different levels of reduction, and (c) results of FE simulation showing the effective strain distribution in the sample forged at 950 °C to 60% reduction. The location from which samples were taken for CTT trials are highlighted with a broken rectangle in (c).

2.3 Cyclic thermal treatments (CTT)

The samples for CTT trials, with a typical dimensions of 13 mm diameter and varying length, were extracted from the forged cylinders using electrical discharge machining (EDM), at locations radially 15 mm away from the centre, as highlighted in Fig. 1c. This was to ensure that all samples have experienced the same thermo-mechanical history and similar strain distribution following the forging process. The extracted samples were skin turned to 12 mm in diameter and cut to a final length of 34 mm (Fig. 1c). To monitor the temperature profile, a K type thermocouple with 1 mm diameter was inserted at the mid height of the samples to a depth of 6 mm (i.e., centre of the sample).

The samples were then coated with delta glaze for oxidation resistance and to minimise heat loss. The samples were then subjected to CTT using both induction and conventional furnace heating methods. The conventional furnace cyclic thermal treatment (FCTT) was considered to achieve a slower heating (i.e., ~ 2.5 °C /min and ~ 10 °C/min) and cooling (~ 1 °C/min and 5 °C/min) rates; the induction cyclic thermal treatment (ICTT) was considered to apply higher heating rates of up to ~ 300 °C/min (Fig. 2b). A total number of 10 cycles was considered for all conditions. The variation in heating and cooling rates had significantly reduced the time duration for CTT from 87600 seconds (i.e., ~ 2.5 °C/min) and 22400 seconds (i.e., ~ 10 °C/min) for FCTT to 720 seconds for ICTT (i.e., ~ 300 °C/min).
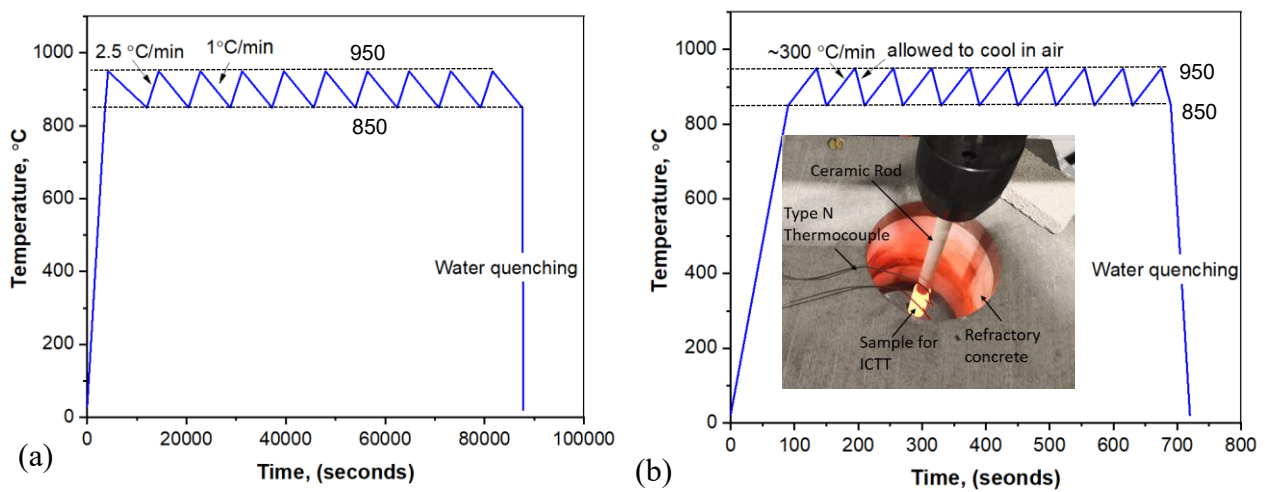

Figure 2: Schematic representation of CTT, (a) using conventional furnace (i.e., FCTT) under a heating rate of ~ 2.5 °C/min and cooling rate of ~ 1 °C/min, and (b) using induction heating (i.e., ICTT) under a high heating rate of ~ 300 °C/min and cooling rate of ~ 8 °C/min. A photograph of the induction heating chamber and a sample with an embedded thermocouple is shown as an insert in (b).

For both methods, samples were initially heated to 850 °C at which the CTT was commenced and employed between 850 °C and 950 °C (Fig. 2). The CTT durations, depending on the heating and cooling rates, were estimated to be ~ 24 hours, ~ 7 hours and ~ 12 minutes for ~ 2.5 °C/min, ~ 10 °C/min and ~ 300 °C/min heating rates, respectively. For the FCTT, the samples with different initial microstructural conditions were treated together under each heating rate, whereas for ICTT the samples were treated individually (Fig. 2b). For all cases, the samples were water quenched after CTT to freeze the microstructure as much as possible.

2.4 Microstructure Characterisation

Microstructure characterisations, using a scanning electron microscopy (SEM), were carried out on the samples in the as solution annealed and in the as hot forged (i.e., at both 1050 °C and 950 °C)

conditions, and following the CTT trials. The samples were dissected in the middle section parallel to the initial forging direction and prepared using standard metallographic technique to a mirror finish condition. The mirror finished samples were then subjected to a final vibratory polishing using 0.2 μm colloidal silica as suspension for 12 hours. Microstructure characterisations were carried out in an FEI Quanta-650 field-emission gun (FEG) -SEM operating at 20 kV. Back scattered electron (BSE) mode micrographs were opted during SEM analysis for microstructural observations. The BSE micrographs were analysed using Leica image analysis software for the measurement of volume fraction of phases and fraction of α globularisation. Three BSE Images with a typical scan area size of 400 × 300 um, covering large number of α grains, were considered for these analyses. For each process condition at least three BSE micrographs were processed to produce statistically representative data. The micrographs were segmented using conventional thresholding image analysis process in Leica image analysis software where all grains were extracted. An ellipse was fitted to each grain whereby the aspect ratio was calculated as the ratio of the major axis to the minor axis irrespective of the crystallographic orientation. The grains with aspect ratio (Major-axis/Minor-axis) less than 3 were considered as globularised, which is a common practice by industry for the measurement of globularisation [11, 12]. Additionally, electron backscatter diffraction (EBSD) maps were acquired from the centre of mid-plane at the high strain zone of selected samples using a fully automated HKL-EBSD system interfaced to the FEG SEM, with an accelerating voltage of 20 kV, 100 μm diameter aperture and a step size of 0.2 μm. In all cases, a minimum of 75% of the scanned areas were indexed.

3.0 Results

3.1 The β solution annealed microstructure

The β phase formed during heat treatment above β transus temperature (i.e., 1020 °C) has transformed to fine martensitic-Widmannstatten microstructure upon water quenching. The Widmannstatten microstructure constitutes lamlellar α plate with thickness of ~ 1 μm and prior β grain size of ~ 300 μm (Fig. 3). The EBSD data revealed the presence of β phase at the plate boundaries, however, its fine distribution has resulted in ~ 4.4 % of unindexed points (Fig. 3b). This microstructure serves as the benchmark for the CTT treated samples.
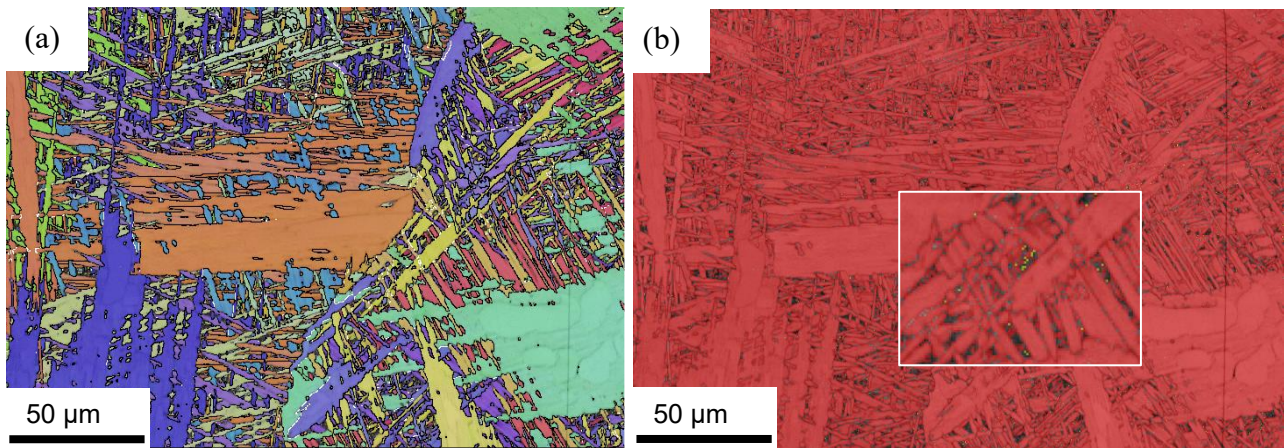
Figure 3: (a) EBSD inverse pole figure (IPF) map showing the fine Widmannstatten microstructure with grain boundaries of secondary α plates, and (b) EBSD phase map showing the fine distribution of β phase at the intergranular regions (yellow colour), poorly indexed.

3.2 Effect of CTT on microstructure evolution

3.2.1 β annealed microstructure

FCTT of the initial β solutioned Widmannstatten microstructure has resulted in coarsening of lamellar α plates during heating and cooling cycles between 850 °C and 950 °C with slow rates (Fig. 4a and b). This has also resulted in coarse primary α grains with average size of ~ 45 μm and ~ 30 μm for ~ 2.5 °C/min and ~ 10 °C/min heating rates, respectively. The increase in heating and cooling rates (i.e., ICTT) affected the evolution of α phase such that more fragmentations of fine lamellar α plates with no significant coarsening was observed (Fig. 4b). This has resulted in fine fragmented α grains of ~ 4 μm and larger primary α grains with average size of ~ 20 μm. The substantial changes in the volume fraction of transformed β and α phase, compared to the initial β solutioned microstructure, is due to the ICTT process.
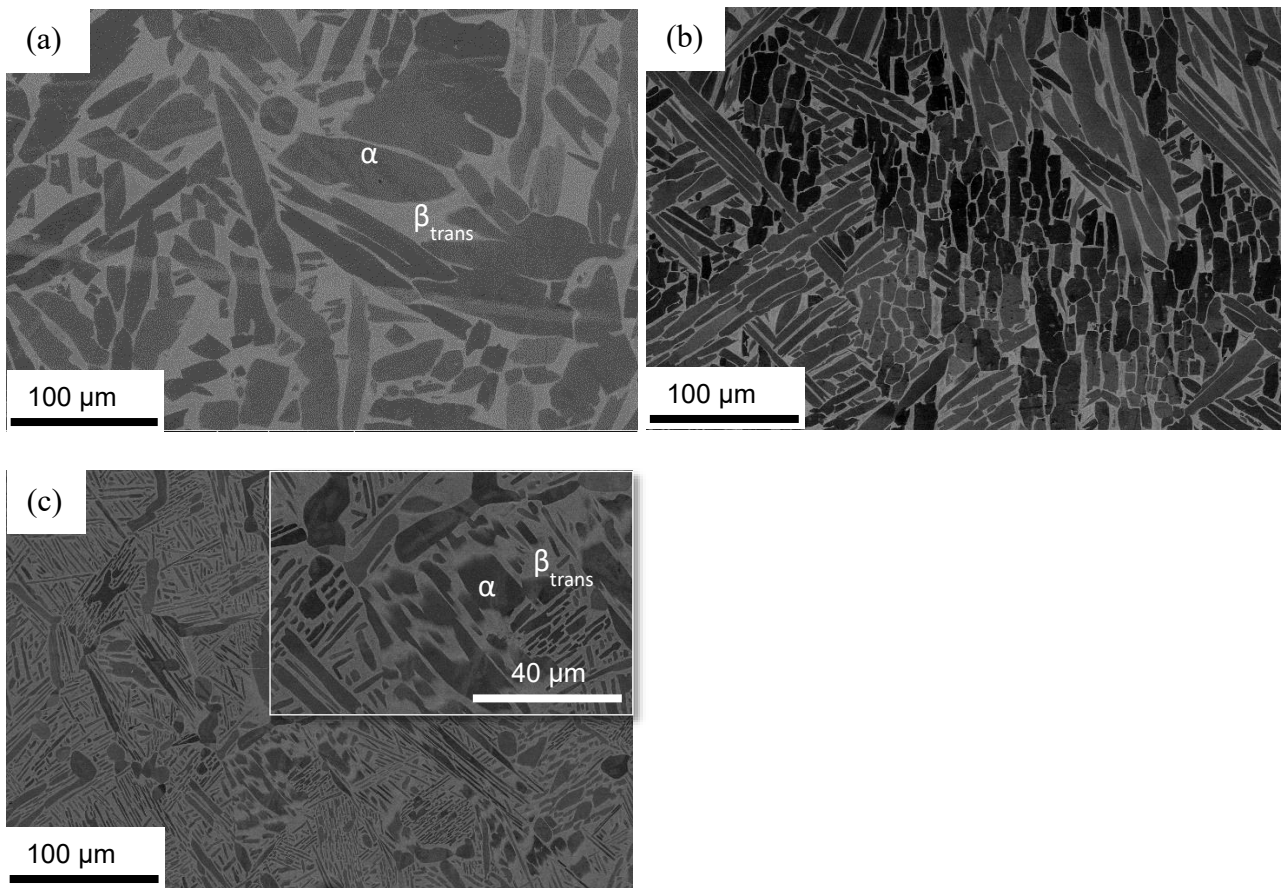
Figure 4: BSE micrographs of the β solution treated microstructure (a) after FCTT under ~ 2.5 °C/min heating rate, (b) after FCTT under ~10 °C/min heating rate and (c) after ICTT under ~ 300 °C/min heating rate. (Higher magnifications insets are provided in (c) for clarity).

3.2.2 β worked at 1050 °C

Hot forging of the initially β solutioned sample at 1050 °C has significantly changed the microstructure characteristics. The sample forged to 60% reduction at 1050 °C revealed long elongated and equiaxed prior β grains with well grown lamellar primary α separated by thin retained β (Fig. 5a) upon quenching. The reduction in temperature during forging and/or after forging below β transus, just before water quenching, has resulted in the growth of lamellar α formed within the matrix of prior-β grains (Fig. 5a).
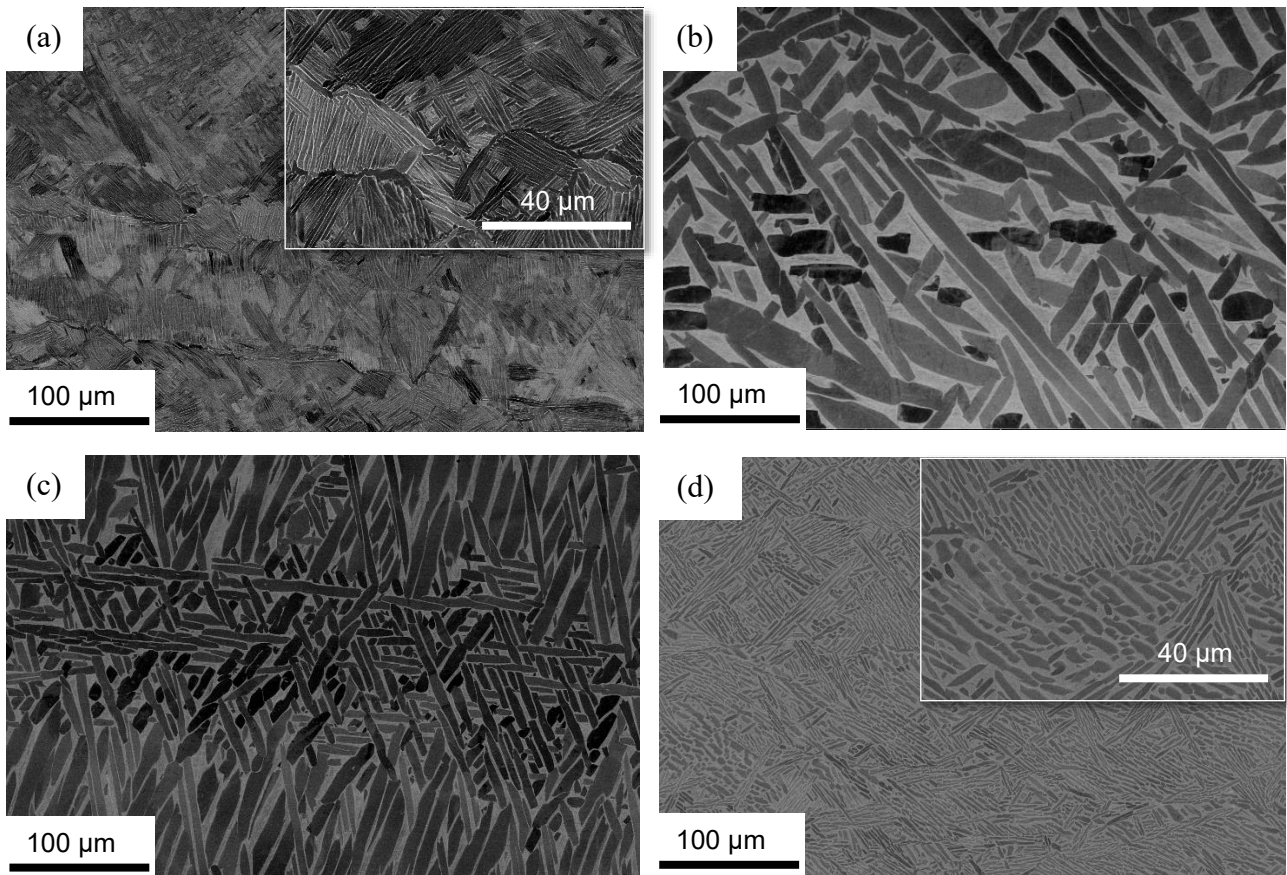
Figure 5: BSE micrographs showing the evolution of microstructure during forging to 60% reduction at 1050 °C and after CTT, (a) the as-forged microstructure (b) after FCTT under ~ 2.5 °C/min heating rate, (c) after FCTT under ~ 10 °C/min heating rate, and (d) after ICTT under ~ 300 °C/min heating rate. Higher magnifications insets are provided in (a) and (d) for clarity.

The very slow heating and cooling rates applied during the FCTT method had a significant impact on the microstructure evolution. The induced strain energy during forging above β transus (i.e., 60% reduction) act as driving force for both α grain refinement and globularisation of primary α during FCTT (Fig. 5b). The increase in heating rate during FCTT has resulted in a decrease in plate thickness and α grains size (Fig. 5c). The ICTT on the other hand has resulted in significantly fine α grains (~ 3.2 μm) with minimum coarsening. However, the globularisation of primary α has still not been completed after CTT. The fragmentation of the initial lamellar α to globular α is clearly evident in Fig. 5. The coarsening under the slow heating/cooling rate (i.e., FCTT) has also led to an increase in volume fraction of transformed β phase from ~ 33% to ~ 52%. The sample subjected to ICTT revealed significant fragmentation of α lamellar to relatively finer α grains and a substantial fraction of transformed β. This suggests the increased response of the microstructural evolution mechanisms to CTT under higher heating/cooling rates following hot work above β transus (Fig. 5c-d).

3.2.3 α+β worked at 950 °C

The β solution treated sample that was forged to 20% reduction at 950 °C (i.e., α+β range) revealed a significant variation in microstructure due to dynamic and post-dynamic recrystallisation of the lamellar α plates (Fig. 6). The as-deformed microstructure consisted of coarse lamellar α lamellar grains with intergranular transformed β (Fig. 6a), in which no significant fragmentation of lamellar α grains was observed.
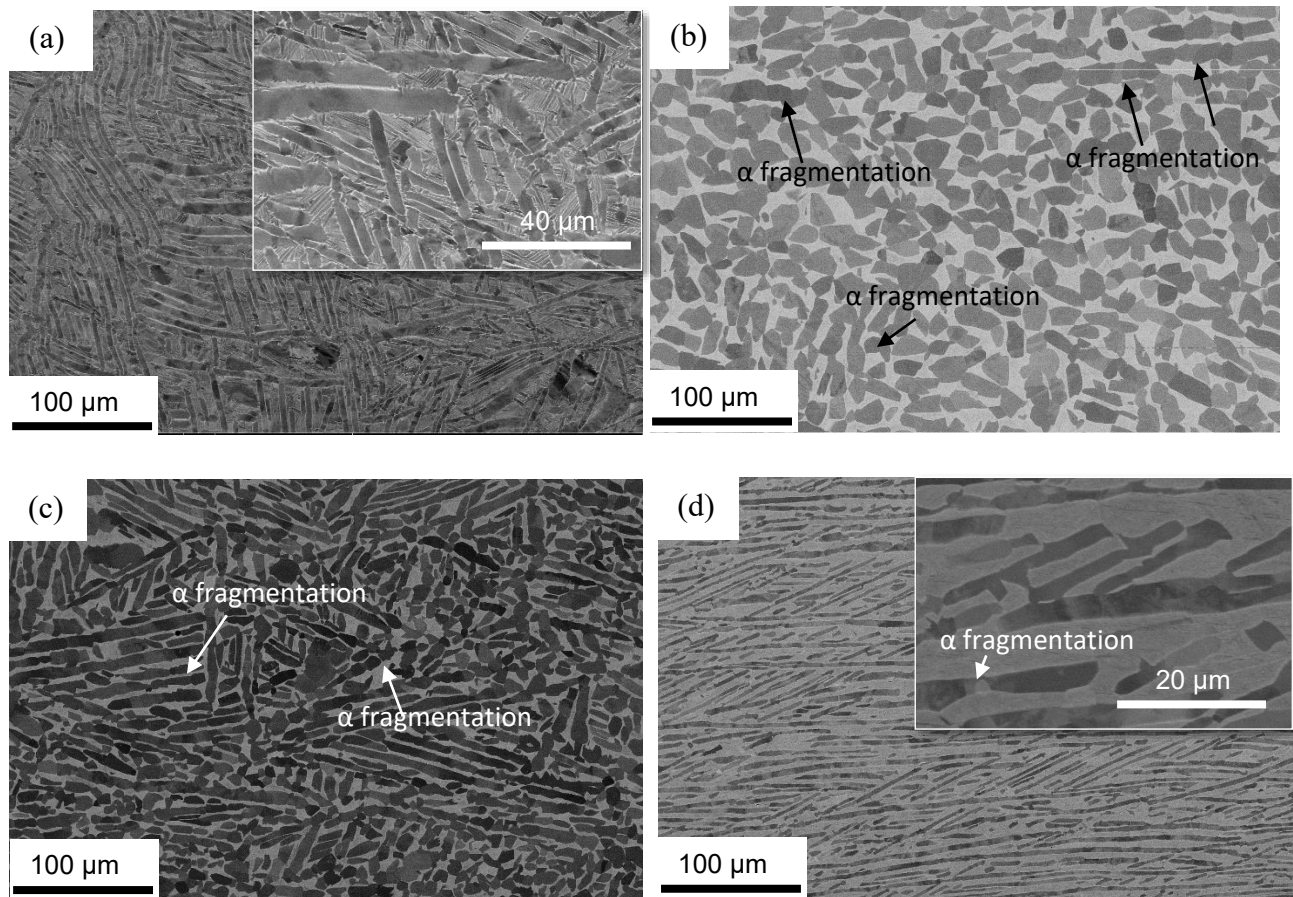

Figure 6: BSE micrographs showing the evolution of microstructure during forging to 20% reduction at 950 °C and after CTT, (a) the as-forged microstructure (b) after FCTT under ~ 2.5 °C/min heating rate, (c) after FCTT under ~ 10 °C/min heating rate, and (d) after ICTT under ~ 300 °C/min heating rate. Insets showing the microstructures at higher magnifications are provided in (a) and (d) for clarity.

The FCTT under the very slow heating and cooling rates (i.e., ~ 2.5/1.0 °C/min), applied on the as forged material (i.e., 20% reduction), has led to the globularisation of the coarse α lamellar by ~ 92% (Fig. 6b). The locations of early stage of α lamellar fragmentation, are highlighted by arrows in Fig. 6b. The average grain size of the globularised α grains was measured to be ~ 16 μm with equiaxed morphology in a matrix of transformed β (~ 35%). These observations suggest that the FCTT is highly effective for microstructural modification of Ti-6Al-4V alloy with small level of hot working at α+β temperature range (i.e., under β transus). An increase in the heating rate from ~ 2.5 °C/min to ~ 10 °C/min during FCTT of the as forged material has reduced the fraction of globularised α grains to ~ 60% (Fig. 6c). Meanwhile, a large number of α lamellar fragmentations, as a result of FCTT, were observed. On the other hand, the fraction of α grain globularisation has further reduced to ~ 35% for the as-forged sample subjected to ICTT under ~ 300 °C/min heating rate (Fig. 6d).

The medium level of applied strain (i.e., 40% reduction) has led to kinking and bending of α lamellae as shown in the micrograph taken from the as-forged condition (Fig. 7a). The microstructure clearly revealed the fragmentation of lamellar α plates due to forging and the formation of intergranular transformed β phase after quenching from 950 °C. The increase in strain (i.e., 40% as opposed to 20% reduction) has also led to the reduction in α lamellae thickness. The BSE micrograph shows complete globularisation of α grains (Fig. 7b) as a result of FCTT. Also, grain coarsening has been observed which occurs because of FCTT under slow heating/cooling rate. The increase in heating rate to 10 °C/min during FCTT has led to lower fraction of α grains globularisation (i.e., up to ~ 80%) and finer size (Fig. 7c). Meanwhile, the ICTT with faster heating/cooling rate has resulted in ~ 55% α grains globularisation fraction with finest equiaxed grains compared to FCTT (Fig. 7d). Overall, higher fractions of equiaxed primary α and transformed β grains, with bimodal distribution, were observed for the samples forged to 40% reduction prior to CTT, suggesting the high potential of this method for globularisation of Ti-6Al-4V with minimised α+β working.
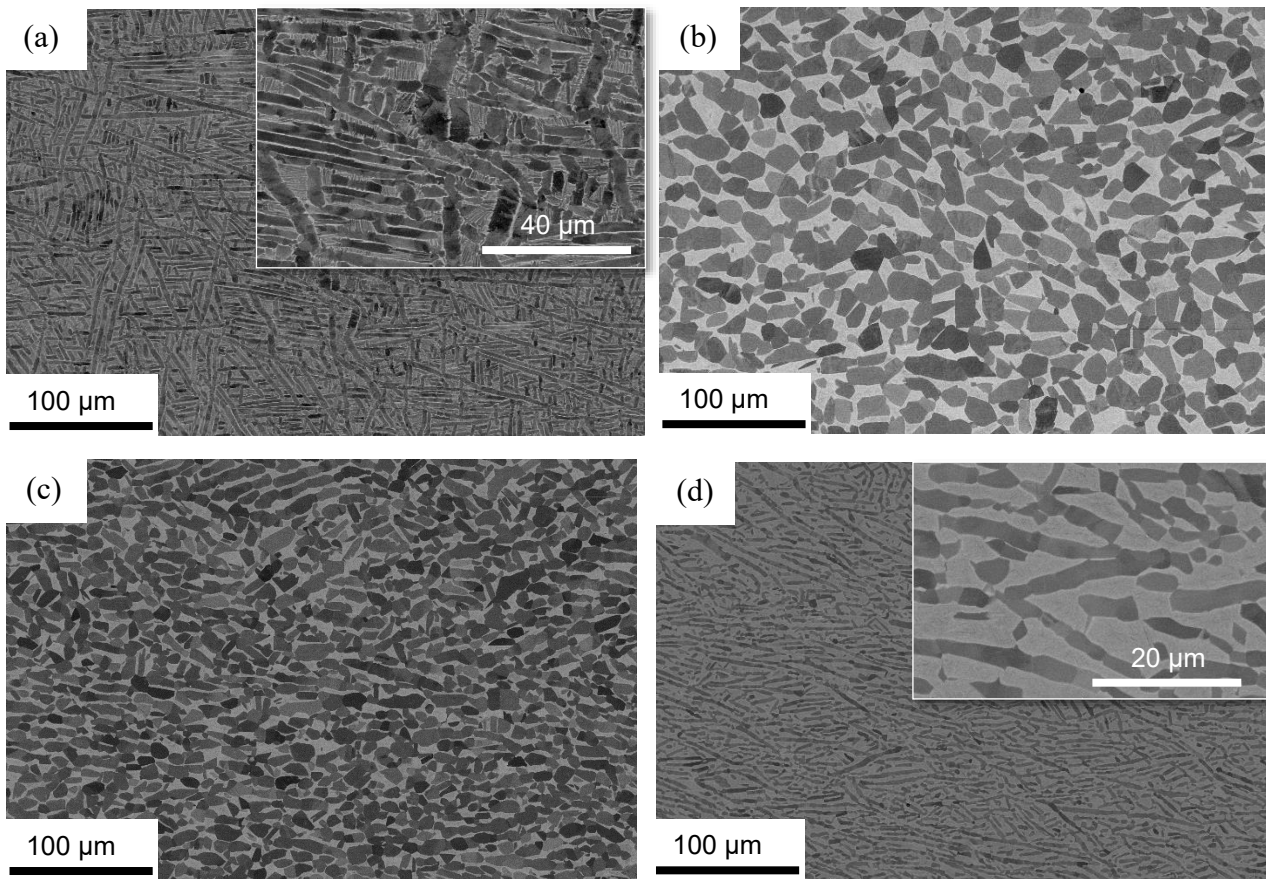
Figure 7: BSE micrographs showing the evolution of microstructure during forging to 40% reduction at 950 °C and after CTT, (a) the as-forged microstructure (b) after FCTT under ~ 2.5 °C/min heating rate, (c) after FCTT under ~ 10 °C/min heating rate, and (d) after ICTT under ~ 300 °C/min heating rate. Insets showing the microstructures at higher magnifications are provided in (a) and (d) for clarity.

The microstructure of the sample deformed to 60% reduction during the α+β working at 950 °C show that the induced strain enhances globularisation of the coarse α lamellae with significant reduction in the transformed β volume fraction (Fig. 8a). The effect that dynamic recrystallisation on the fragmentation of the lamellar α to fine α grains is clearly observed. The CTT has altered the microstructure drastically, irrespective of the heating/cooling rates and the method (i.e., FCTT and ICTT). The FCTT had resulted in complete α grains globularisation in the as-forged microstructures under both implemented heating/cooling rates (i.e., 2 °C/min and 10 °C/min) (Fig. 8b & c). The ICTT, on the other hand, led to ~ 85% globularisation of α grains with maximised fragmentation (Fig. 8d). These significant changes in the microstructures observed after conducting CTT on samples subjected to higher level of strain (i.e., 60%) suggest that both FCTT and ICTT can be effectively used for globularisation. Additionally, a combination of large deformation during forging and the faster heating/cooling rates applied during ICTT resulted in fine α grains implying that ICTT can potentially

be used for manufacturing parts with fine grain size to enhance super-plastic forming or to increase mechanical properties [13].
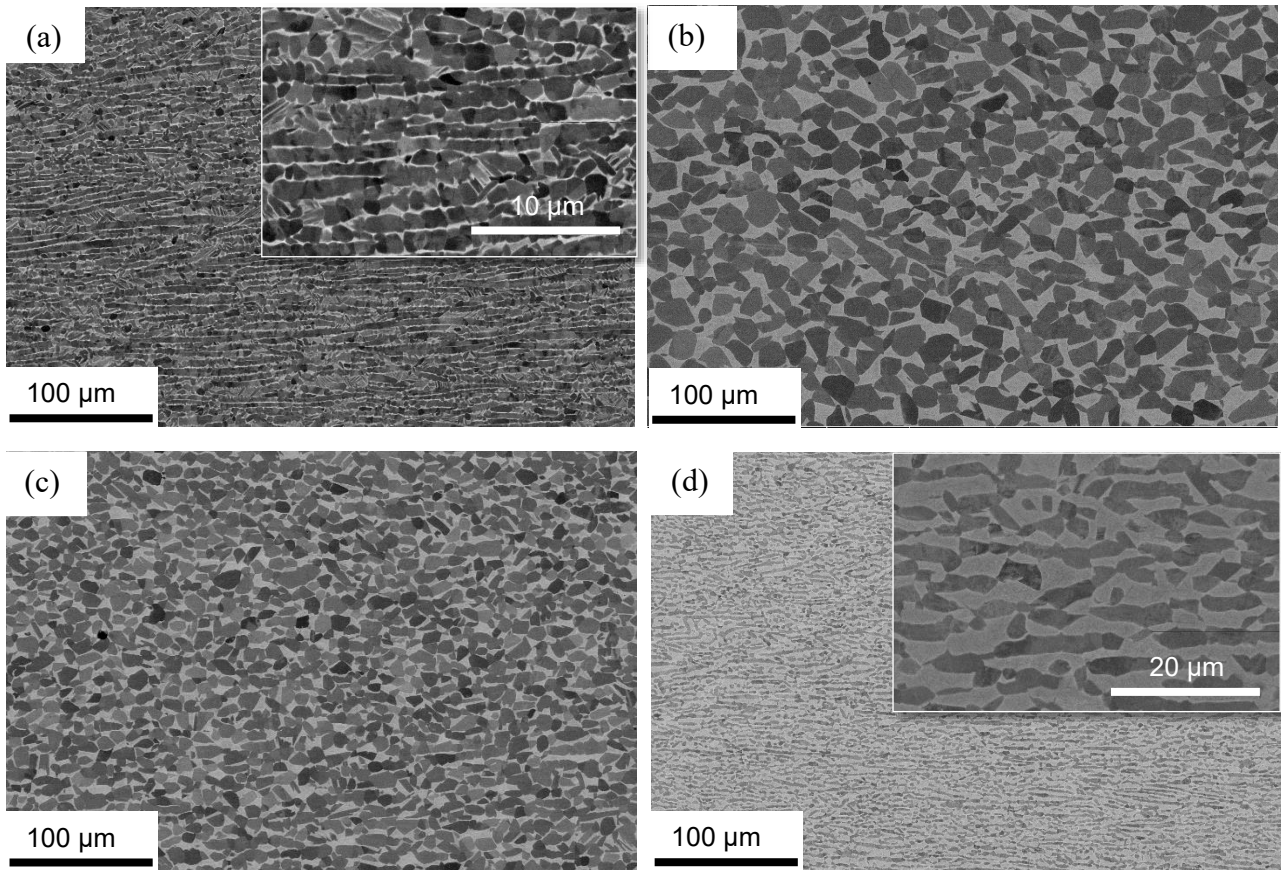

Figure 8: BSE micrographs showing the evolution of microstructure during forging to 60% reduction at 950 °C and after CTT, (a) the as-forged microstructure (b) after FCTT under ~ 2.5 °C/min heating rate, (c) after FCTT under ~ 10 °C/min heating rate, and (d) after ICTT under ~ 300 °C/min heating rate. Insets showing the microstructures at higher magnifications are provided in (a) and (d) for clarity.

The average α grain size for the samples forged at the sub-transus temperature (i.e., 950 °C) was 4.7 μm, 3.4 μm and 2.7 μm, respectively for 20%, 40% and 60% reductions (Fig. 6a, 7a & 8a). Whereas, the average α grain size measured for the forged samples subjected to FCTT under slow heating rate (i.e. 2.5 °C/min) ranged from 11.6 μm for 60% to 16.2 μm for 20% reductions (Fig. 6b, 7b & 8b). The significant coarsening observed is to the slow cooling rate during the FCTT process which provides enough time for grain growth. On the other hand, the average α grain size measured for samples subjected to ICTT (i.e. ~ 300 °C/min heating rate) ranged from 2.8 μm for 60% to 5.8 μm for 20% reductions (Fig. 6d, 7d & 8d). This shows the higher efficiency of ICTT over the FCTT to develop finely equiaxed α grain. Though, the sample subjected to ICTT shows relatively less globularisation fraction compared to those of the samples subjected to FCTT samples. This suggests that FCTT is more effective for globularisation while ICTT for achieving fine α grains. Therefore, to

achieve a globularised microstructure with fine α grains, a combination of both FCTT and ICTT (i.e., a sequence of slow and fast heating/cooling rates) can be effective.

4.0 Discussion

The microstructural evolution leading to globularisation of α grains in Ti-6Al-4V alloy is typically done through consecutive thermal and mechanical treatments comprising of sequential deformation and static heat treatments [14]. The initial stage of α grain globularisation is driven by hot deformation where the activation of different slip systems and the generation and evolution of dislocations lead to the onset of fragmentations in α grains [15]. Whereas, the static heat treatment processes have relatively minimum impact on the dislocations evolution as compared to hot deformation [16]. The observed variation in the as-forged microstructures, suggests the significant influence of strain and temperature on microstructure evolution. The substantial fragmentations of primary α laths to globular α grains with increasing the level of reductions indicates that the strain magnitudes applied during forging at both sub-transus and above β transus temperature accelerates the globularisation kinetics (Fig. 8). The increase in strain during the α+β working lead to fine α grains, which can be related to the increase in dynamic recrystallisation [10].

The extent of α lamella fragmentations and the formation of substructures within primary α grains and β matrix had significant impact on the fraction of α globularisation during CTT. However, the relatively lower fraction of α globularisation obtained for the samples forged above β transus can be related to the stress relaxation occurred upon cooling from the forging temperature (i.e., above the β transus) which lowers the driving force required for globularisation. The measured fractions of globularisation for varying initial material conditions (i.e., different initial forging) suggest that maximum level of globularisation in α grains can be achieved with higher level of deformation at sub-transus temperature (i.e., at 950 °C) (Fig. 9). Despite a relatively lower effectiveness compared to other cases in this study, but the extent of α grain globularisation measured for the sample deformed to 20% reduction at sub-transus temperature after CTT suggest that this technique can be considered as an effective route for industrial applications.
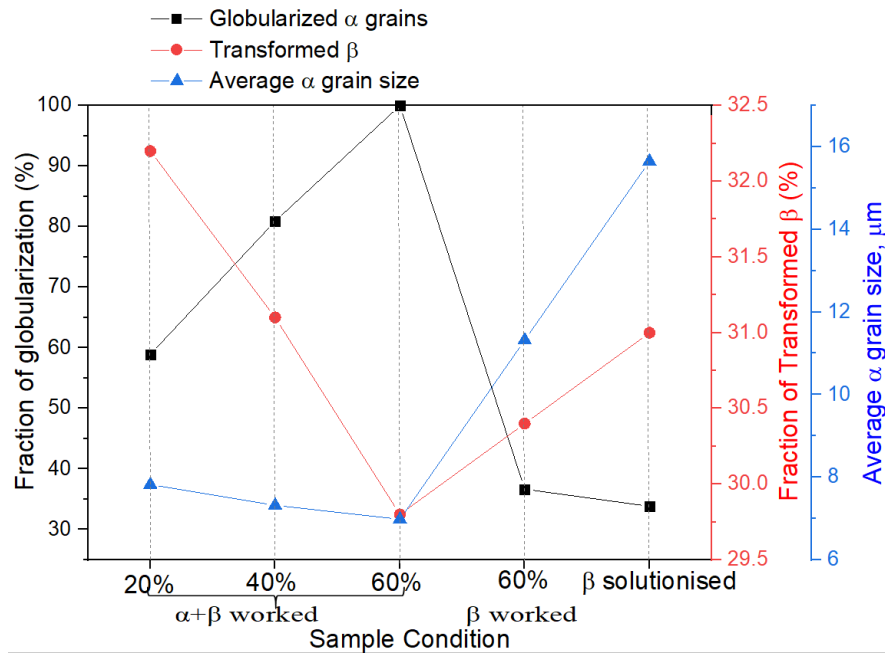
Figure 9: Effect of FCTT at heating rate of 10 °C/min on microstructure characteristics in materials deformed to different levels of deformation, compared to β solutionised microstructure.

The sufficient time during heating/cooling available for the diffusion assisted substructure evolution resulted in maximum fraction of α grain globularisation after FCTT as compared to ICTT (Fig. 10). The relatively quicker heating/cooling rates applied during ICTT (i.e., ~ 720 s overall process duration) was not sufficient enough to complete the globularisation of the partially fragmented lamellar α grains for the case of samples treated after 60% reduction. Further, the slow cooling and associated coarsening of α grains led to substantial reduction in volume fraction of transformed β in the samples subjected to FCTT. On the other hand, the very fast cooling experienced by the samples subjected to ICTT led to finer α grains with ~ 20% increase in the volume fraction of transformed β, irrespective of the initial deformation conditions. This suggest that the volume fraction of β existed at 950 °C had not changed significantly during the cooling stage of ICTT, and resulted in higher fraction of transformed β (Fig. 10).
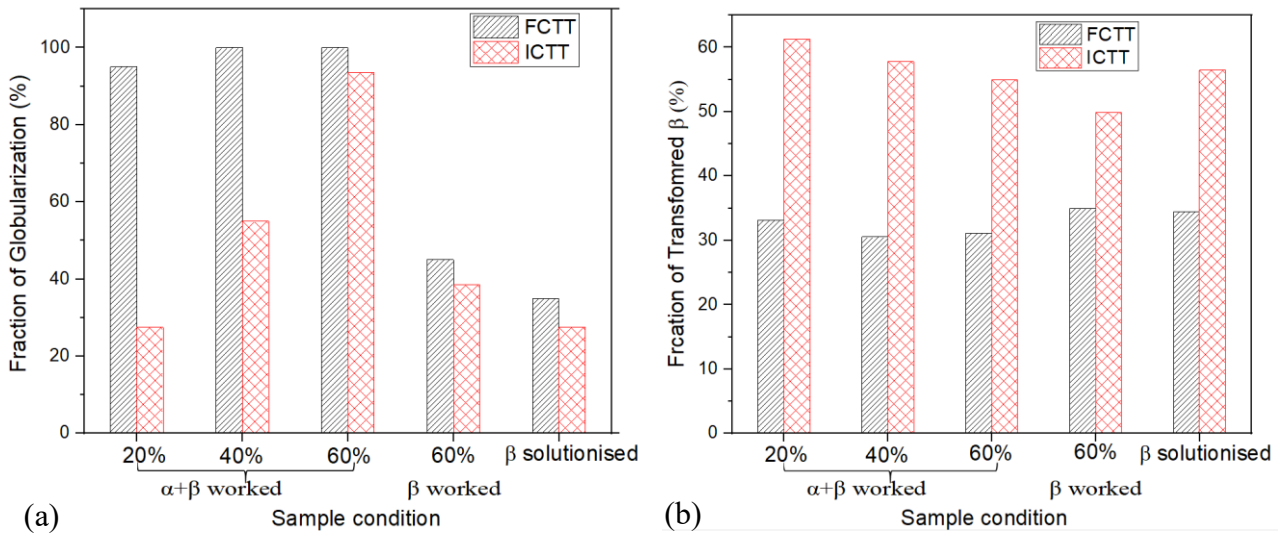
Figure 10: Histogram showing the variation in (a) the fraction of globularised α, and (b) the fraction of transformed β, formed in the samples with different starting microstructures for both FCTT (heating rate ~ 2.5 °C/min) and ICTT (heating rate ~ 300 °C/min).

4.1 Globularisation mechanisms

The volume change associated with the allotropic phase transformation of titanium alloys from α to β phase during heating led to an internal work hardening [17]. However, the low level of work hardening generated during simple heat treatment is not sufficient enough to refine the α grain structure [9]. The effect of work hardening mainly depends on the heating rate adopted and the complexity of heating cycles. Therefore, the volume change during CTT can generate significant plastic micro strains as result of internal work hardening. This upon further heating results in active strain recovery mechanisms within the material. Thus, the CTT can significantly contribute to vacancy generation and annihilation of defects to form low angle grain boundaries and substructures within the existing α grains. Further, the change in volume fraction of β phase during CTT results in nucleation of new β phase in between the α grain boundaries [6]. Hence, the two major factors which trigger glubularisation during CTT of α lamellae are the number of point defects generated and an appropriate temperature above recrystallisation (~ 750 °C).

To understand the fragmentation mechanism, misorientation analyses were carried out on 5 different α lamellae (Fig. 11a). The measured disorientation profiles for the selected α lamellae show the progressive evolution of globularisation during CTT (Fig. 11b). The disorientation profile of lamella 5 with small step changes in misorientation angles (i.e., <10) indicates the early stage of fragmentation and local rotation of small globularised α grains inside the α lamella; whereas the distinct step changes in the disorientation profile of lamella 1 with >30° misorientation angle per step is the indication of the completion of globularisation in this lamella. The disorientation profiles for

other lamellae (i.e., 2, 3, and 4) show that the progress of globularisation are in between those of lamellae 5 and 1. An increase in the misorientation relative to the first point for α grains with various orientations suggest that continuous crystal rotations inside the fragmented α lamellae during the implemented CTT (Fig. 11 b).
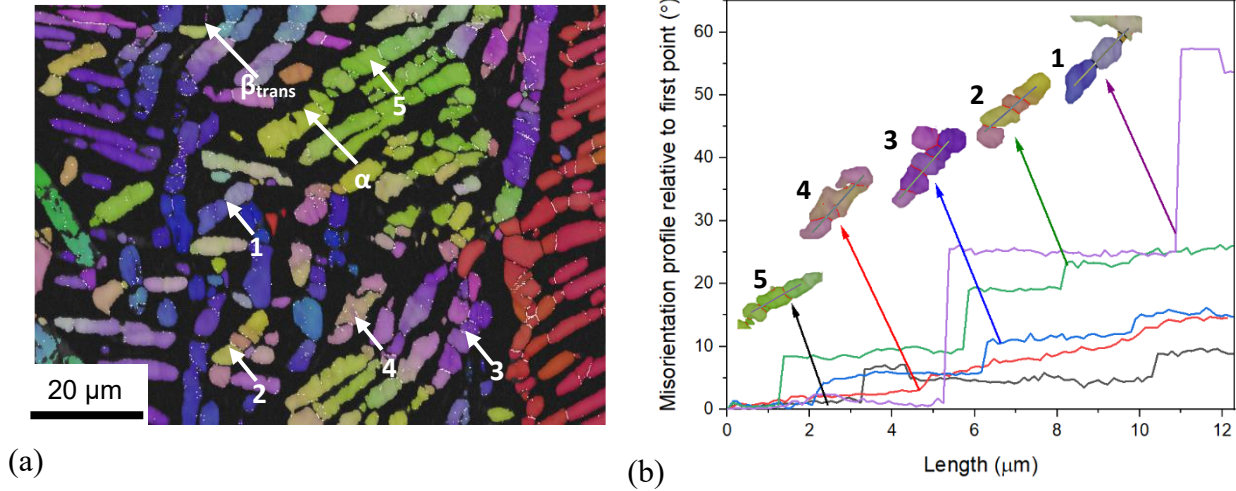

Figure 11: a) EBSD IPF map showing the fragmentations of α grains and transformed β matrix (black regions) in a sample forged to 20% reduction followed by ICTT under ~ 300 °C/min heating rate, and (b) plots disorientation profie inside selected α-lamellae highlighted in (a)., relative to the first point, showing the progress of fragmentation and globularisation.

There are different mechanisms active during the globularisation process including (i) cylinderisation, (ii) edge spheroidisation, and (iii) boundary splitting followed by thermal grooving (i.e., termination migration) [6]. The formation of curved edges at either sides of α lamellae leading to mass transfer from the edges to the flat regions and formation of globular grains is known as the cylinderisation [18]. The formation of curved edges similar to cylinderisation and separation of spheroids from the edges by perturbations is known as the edge spheroidisation. On the other hand, the formation of sub-grain boundaries within the lamellar α grains leading to the fragmentation of secondary α and nucleation of β phase at grain boundaries due to diffusion, resulting in the transformation of sharp edges to round globular grains, is known as boundary splitting followed by thermal grooving [6].

A combination of edge spheroidisation and boundary splitting followed by thermal grooving observed in micrographs of the samples forged to 60% reduction at 1050 °C (i.e., above β transus) suggest high potential of these microstructures for globularisation after FCTT and ICTT (Fig. 12a and b). However, the strain recovery due to phase transformation from above β transus has significantly reduced the fraction of globularisation. On the other hand, the pre-CTT forging at 950 °C (i.e., α+β region) has revealed boundary splitting followed by thermal grooving as the dominant

mechanisms after both FCTT and ICTT (Fig. 12 c & d). No evidence for cylinderisation was observed under any of the conditions studied.
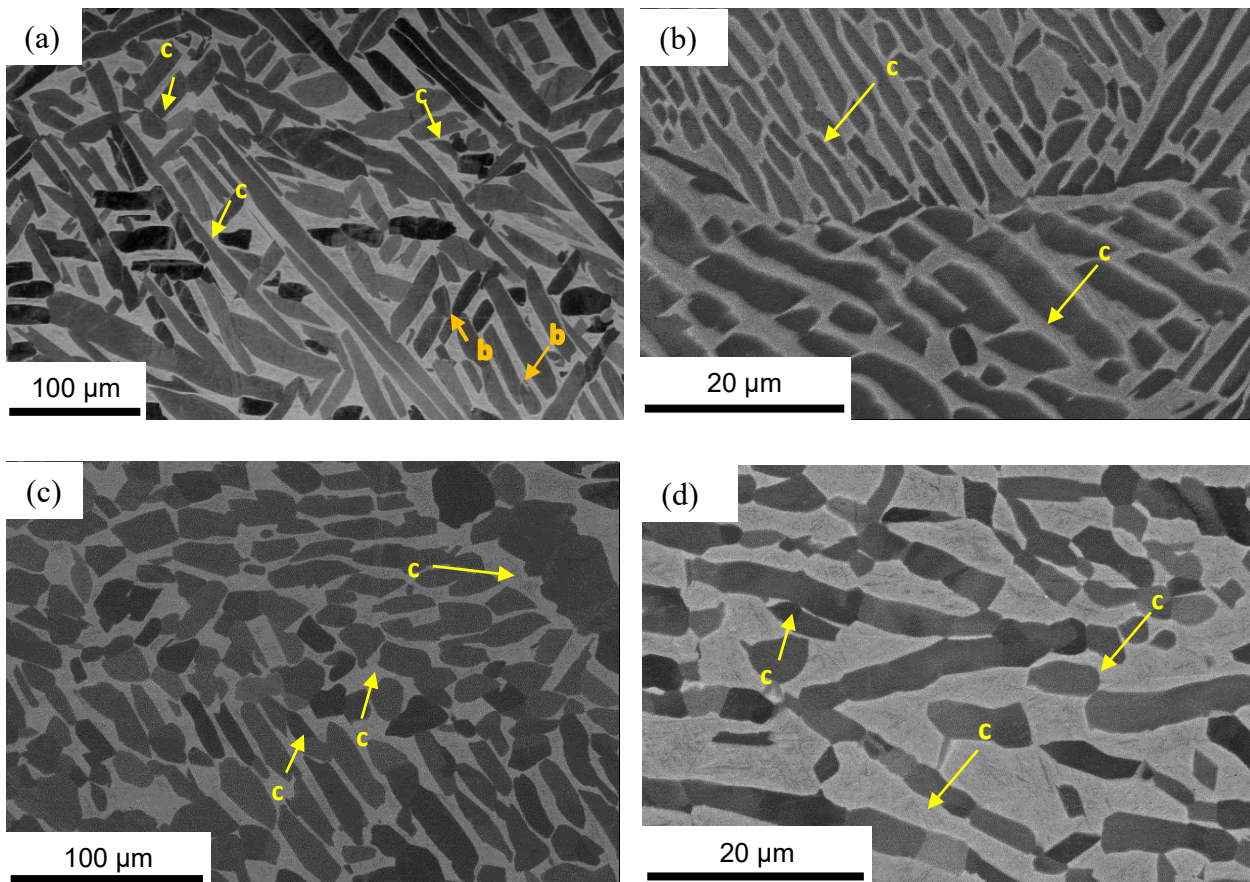

Figure 12: BSE micrographs showing the progress of glubularisation in primary α lamellae, (a) β worked to 60% reduction and subjected to FCTT under ~ 2.5 °C/min heating rate, (b) β worked to 60% reduction and subjected to ICTT under ~ 300 °C/min heating rate, (c) α+β worked to 20% subjected to FCTT under under ~ 2.5 °C/min heating rate and d) α+β worked to 20% subjected to ICTT under ~ 300 °C/min heating rate. (Arrows marked are b= edge spheroidisation and c = Boundary splitting followed by thermal grooving).

4.2 Kinetics of microstructure evolution

The kinetics of static globularisation during CTT has been evaluated by taking into consideration of the strain, temperature, time and heating rate. The globularisation kinetics has been described in the form a constitutive equation that has been implemented in the DEFORM® software as a user sub-routine to predict microstructure evolution.

The globularisation Ti-6Al-4V alloy during CTT is considered as a diffusion controlled process in which vacancy formation and substructure evolution are the main driving mechanisms. The Johnson-Mehl-Avarmi-Kolmogorov (JMAK) equation for recrystallisation was adopted, which

has successfully been used for predicting recrystallisation in Ti-6Al-4V alloy [12]. The JMAK equation describing the fraction of static globularisation (f) as function of time (t) is as below,

$$f = 1 - \exp(-kt^n) \qquad (1)$$

in which, k and n are a constant for globularisation rate and Avrami exponent, respectively. Equation 1 considers the static globularisation as a function of time only. Whereas, the static globularisation can significantly be influenced by the strain magnitude (ε) and temperature (T) [19]. Therefore, to consider these, a $t_{0.5}$ parameter (i.e., the time required for 50% globularisation) is introduced into Equation 1 as below.

$$t_{0.5} = A\varepsilon^{-a}Z^m\exp\left(\frac{Q}{RT}\right) \qquad (2)$$

where, A is material constant, a and m are constants, Z is the Zener Holloman parameter, Q is the activation energy for globularisation in the $\alpha+\beta$ phase region (156 kJ/mol), and R is the global gas constant. Thus, the modified JMAK equation can be re-written as,

$$f = 1 - \exp\left[-k\left(\frac{t}{t_{0.5}}\right)^n\right] \qquad (3)$$

Substituting Equation 2 in Equation 3 yields,

$$f = 1 - \exp\left[-k\left(\frac{t}{A\varepsilon^{-a}Z^m\exp\left(\frac{Q}{RT}\right)}\right)^n\right] \qquad (4)$$

Upon taking logarithm from both sides and substituting $Z = \dot{\varepsilon}\exp(\frac{Q}{RT})$, Equation 4 can be re-written as,

$$\ln\left(\ln\frac{1}{1-f}\right) = n\ln\varepsilon^a + n\ln t - \frac{(m+1)nQ}{RT} + \ln k - n\ln A - mn\ln\dot{\varepsilon} \qquad (5)$$

Thus, Equation 5 accounts for ε, $\dot{\varepsilon}$, T, t, which are the main factors affecting the static globularisation kinetics. To simplify the equation further, the strain rate is considered constant and the material constants (i.e., A, a and m) are normalised to unity. Considering constant a = 1, $n\ln\varepsilon^a$ and $n\ln t$ in Equation 5 can be merged into $n\left(\ln(\varepsilon t) - \frac{2Q}{RT}\right)$, where the strain($\varepsilon$), temperature and heat treatment time (t) are taken into consideration. Additionally, to consider the effect of temperature and further simplify the relationship, Equation 5 has been converted into a linear equation between $\left(\ln\frac{1}{1-f}\right)$ and $\ln\varepsilon t - \frac{2Q}{RT}$ (Fig. 13a). The data reported in literature for globularisation of Ti-6Al-4V have been used to find the linear fit (Fig. 13a) [3, 20, 21].

$$f = 1 - \exp[-exp(0.717 \, (\ln \varepsilon t - (2Q/RT)) - 1.1102)] \qquad (6)$$

Thus, the fraction of globularisation during CTT of Ti-6Al-4Vcan be calculated using Equation 6. The predicted globularisation fraction has been compared with the experimental data from literature [3, 20, 21] for varying strain, temperature and time. A prediction accuracy of ~ 90% obtained for such a large range of temperatures, strains, and time suggesting the suitability of the model for predicting the fraction of globularisation (Fig. 13b).
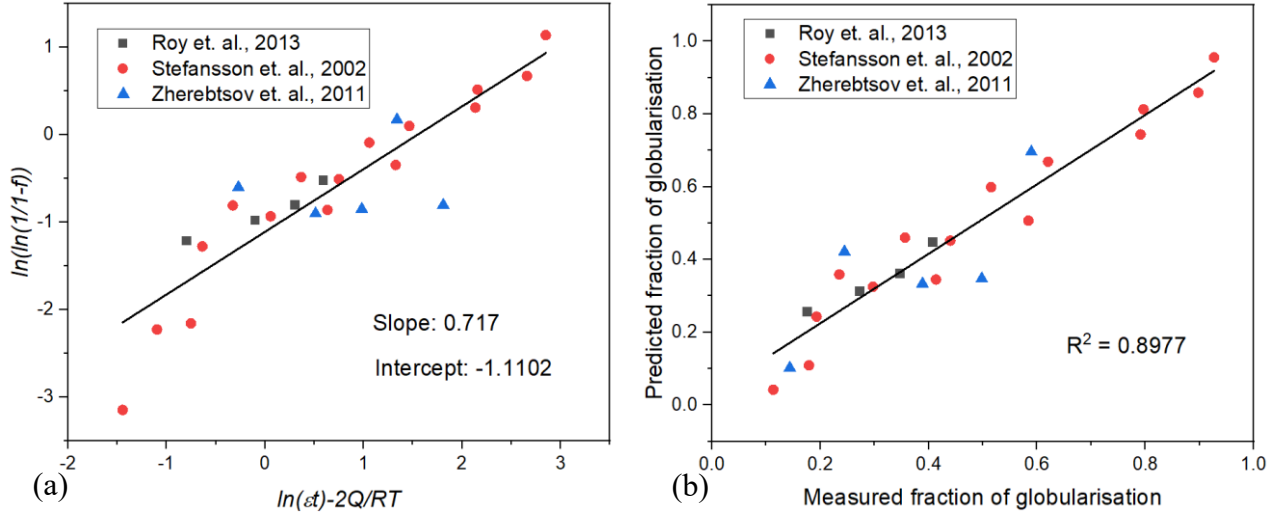

Figure 13: (a) The linear relationship between $\left(ln\frac{1}{1-f}\right)$ and $\ln \varepsilon t - \frac{2Q}{RT}$, and (b) comparison between the results of constitutive model (i.e., Equation 6) predictions and the measured fractions of globularisation in Ti-6Al-4V reported in literature under varying process conditions including: temperatures: 700, 800, 953 °C; strain: 0.35, 0.49, 0.8, 1.1, 1.5, 1.9, and heat treatment time: 0.25, 0.5, 0.75, 1, 2, 3, 4, 5, 6, 8, 13.5 hrs.

Equation 6 is suitable for predicting the fraction of globularisation during heat treatments and therefore can be adopted for the prediction of globularisation during cyclic heat treatment in furnace (i.e., FCTT), which is under slow heating and cooling rates. Whereas, to predict the globularisation during ICTT, which is under relatively higher heating and cooling rates, a multiplication factor of 1.2 for globularisation has been assumed on the basis of experimental fraction measured from the samples subjected to ICTT. Therefore, Equation 6 for induction heating shall be rewritten as:

$$f = 1 - \exp[-exp(0.83 \, (\ln \varepsilon t - (2Q/RT)) - 1.124)] \qquad (7)$$

The results of microstructural analyses suggest that the fragmented α grains (i.e., during initial forging) experienced grain growth to different extent depending on the applied heating and cooling rates during CTT. The driving force for grain growth is the reduction in energy associated with the decrease in grain boundary area. Therefore, the change in grain size due to boundary migration is calculated using the equation below:

$$D - D_0 = Kt^n \tag{8}$$

where, D is the grain size at a certain time, D_0 is the initial grain size, t is the heat treatment time, n is the grain growth rate constant, and K is a constant which depends on the alloy chemical composition and the heat treatment temperature [22].

Assuming that atomic diffusion along grain boundaries is active during grain growth, K can be calculated as the following:

$$K = K_0 \, exp(-Q/RT) \tag{9}$$

where, K_0 is the grain growth exponent, Q is the activation energy for grain growth (250 kJ/mol [23]), R is the global gas constant, and T is the temperature.

The grain growth exponent K_0 has been obtained based on grain size, temperature and time data reported in [24] according to the equations below:

$$D - D_0 = K_0 \, exp(-Q/RT)t^n \tag{10}$$

$$K_0 = \frac{D - D_0}{exp(-\frac{Q}{RT})t^n} \tag{11}$$

The variation in calculated values for K_0 with varying temperature and time ($T{\times}t$) is therefore considered using the linear fit to the Equation below (Fig. 14a):

$$\log K_0 = -0.2277 \times \log(T \times t) + 0.3494 \tag{12}$$

To consider the variation in grain growth rate constant (n) with temperature, n has been calculated as a function of temperature using data presented in [24] fitted to the Equation below:,

$$n = 4 \times 10^{-9} \times T^3 - 1.232 \times 10^{-9} \times T^2 + 0.013 \times T - 4.2175 \tag{13}$$

Thus, the grain growth during CTT was calculated using Equation 8 for varying process conditions. The calculated grain growth has been compared with experimentally measured data reported in literature [24] and a good level of agreement was obtained for grain growth during α+β heat treatment of Ti-6Al-4V with R^2 value of 0.9725 (Fig. 14b). These calculated globularisation and grain growth has been compared with the results from actual CTT samples and discussed in the following section.
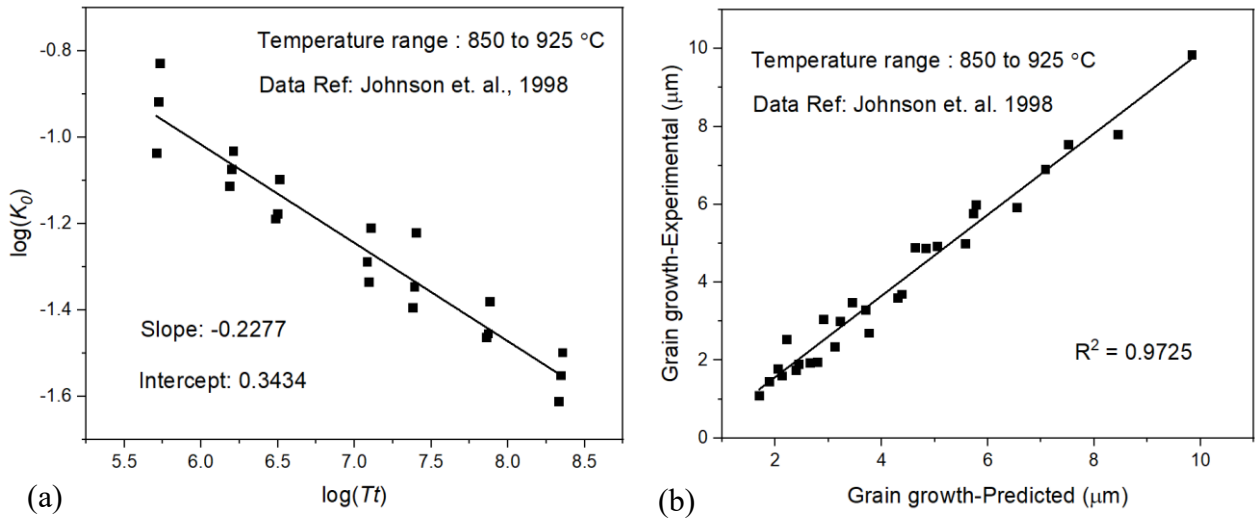
Figure 14 : (a) A linear relationship between log (K_0) and log (Tt) and (b) Comparison between the predicted grain growth based on Equation 8 and the experimentally measured grain growth for Ti-6Al-4V alloy for data reported in [24].

4.3 FE simulation of forging and CTT

The developed JMAK material model for recrystallisation and grain growth was incorporated into the commercially available DEFORM® software package as a post-processing user subroutine. This was to predict the evolution of globularisation and grain growth of primary α grains during CTT implemented in this study on samples forged to three levels of reduction (i.e., 20%, 40% and 60%) at α+β phase temperature (i.e., 950 °C). A non-isothermal hot open-die forging process simulation was created considering a workpiece with similar dimensions as those used for the forging trials (i.e., 85 mm diameter and 85 mm length), using material properties for Ti-6Al-4V available in DEFORM database. The workpiece was meshed with tetrahedral elements to an average mesh size of 1.5 mm at the edges and 4 mm in the centre. The workpiece was soaked at the forging temperature of 950 ˚C, followed by 10 seconds transfer in air to replicate the sample transfer from the furnace to the forging press by applying heat transfer coefficient of 0.02 N/sec/mm/C for air. The friction between the dies were considered as lubricated hot forging condition with coefficient of friction (μ) of 0.3 and convection coefficient 2 N/sec/mm/C for dies. The temperature of the top and bottom dies were kept at ~ 400 ˚C. The top die movement was considered constant with an average speed of 6mm/s (Fig. 15a). The temperature and strain distribution of sample forged to 60% reduction at 950 °C suggest that the maximum temperature and strain magnitude were achieved at the core of the workpiece (Fig. 15b & c).
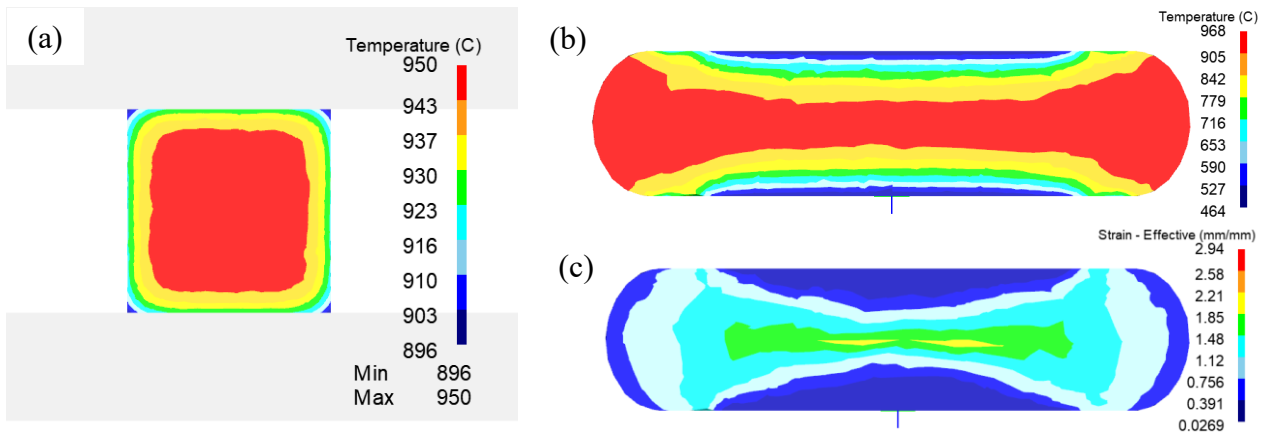
Figure 15: Results of FE simulation showing (a) temperature distribution in the workpiece just before the commencement of forging at 950 °C, (b) temperature distribution in the workpiece after forging to 60% in reduction, and (c) strain distribution in the workpiece after 60% reduction.

Considering the variation in strain distribution, the samples for CTTs were extracted 15 mm away from the centre of the forged sample. To replicate the experimental trials and extract samples similarly from the simulated forged cylinders for CTT, data interpolation method was adopted. For this purpose, a new part with 12 mm diameter and 34 mm height was created and the data form the forging simulation was interpolated to the new part to fix the initial conditions for the simulation of the CTT trials. An example of effective strain distribution taken from the results of forging simulation and being mapped on a new model, for the initiation of CTT simulation (Fig. 16a). The model has then been subjected to CTT conditions for the simulation of ICTT and FCTT. The heating/cooling rates implemented during experimental trials were applied as boundary conditions for the simulation of both treatments. The slower furnace heating and cooling conditions resulted in uniform temperature distributions within the furnace and in samples subjected to FCTT.

The 2D Boundary Element Method (BEM) available within DEFORM was used for 2D axi-symmetric induction heating simulation, in which the requirement to mesh the air between the coil and sample can be ignored (Fig. 16b). The material data base for Ti-6Al-4V has been updated with the electrical resistivity and magnetic permeability values from reference [25]. A constant frequency of 93000 hertz and current density of 6.3 A/mm^2 were considered to achieve the required heating rate. During the ICTT, the samples were allowed to cool in air following the heating cycle, whereby the cooling duration for each cooling cycle was controlled by monitoring the temperature at the core reaching 850 °C. Note that an N-type thermocouple was inserted in each sample to control temperature during each cycle. Finally, after 10 consecutive cycles between the specified temperatures, the samples were then water quenched by applying a heat transfer coefficient of 5 N/sec/mm/C. A significant variation in temperature was noticed between the core and the surface of

the sample in the simulation carried out for ICTT (Fig. 16b). Meanwhile, the temperature of the core region was considered as the point of interest for the prediction of microstructure evolution.

The experimentally measured temperature profiles during CTT were compared with those of the simulated CTT for both FCTT and ICTT (Fig. 16c and d). The simulated temperature profile for FCTT matches well with the measured profile suggesting that the slower heating/cooling cycles lead to a uniform temperature distribution within the sample (Fig. 16c). On the other hand, the faster heating and cooling rates during ICTT introduced marginal variations in the measured and simulated temperature profiles, which can be due to the manual control adopted for controlling the heating rate during ICTT (Fig. 16d). Despite the variation in the simulated and measured temperature profiles, the magnitude and trend are closely matching with negligible uncertainty.
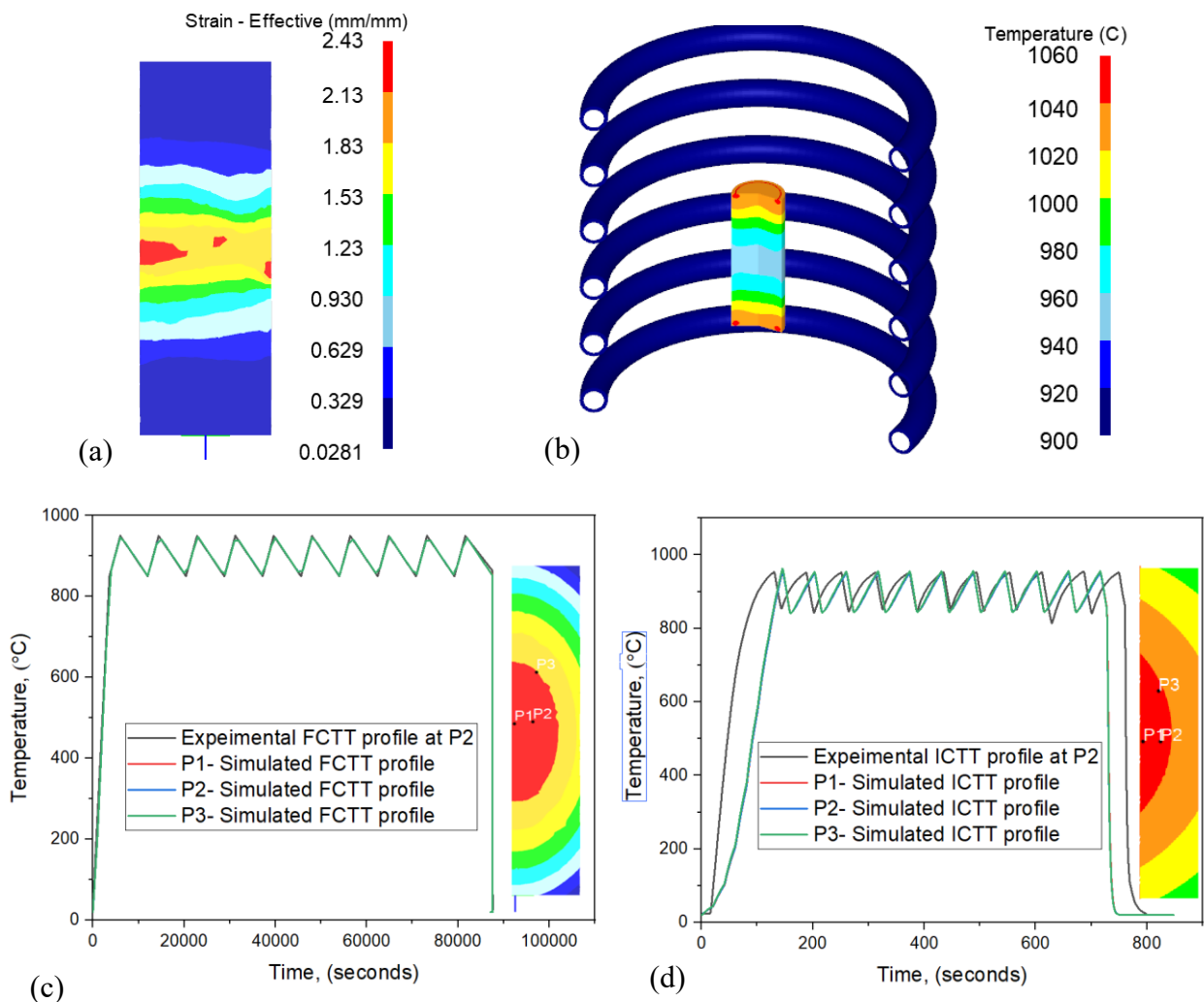

Figure 16: (a) Initial strain distribution mapped for the CTT simulation of sample forged to 60% reduction in the α+β phase region (b) 3D view of induction coil set up and temperature distribution during ICTT, and plots showing measured temperature profile from location close to P2 and predicted temperature profile from three (P1, P2 and P3) locations for c) FCTT and d) ICTT.

4.4 Calibration of the globularisation and grain growth model during CTT

The simulated FCTT on all samples forged in the α+β phase region resulted in 100% globularisation of primary α-grains, which led to the difficulty in comparison between the effect of strain magnitude on globularisation. Therefore, to understand the effect of pre-forge deformation level (i.e., prior to CTT) on the progress of globularisation, the results of FCTT simulations were compared at an intermediate step of after 9000 seconds. The results of simulations show that the core of the sample forged to 60% has reached maximum globularisation (i.e., 100%) after 9000 seconds which is equivalent to 90 minutes of heating above 750 °C (Fig. 17a). The data also show that the core of the sample pre-forged to 40% reduction underwent significant globularisation compared to the sample subjected to 20% reduction where only a fraction of globularisation is achieved after 9000 seconds (Fig. 17b and c). The simulation show that these samples (i.e., pre-forged to 20% and 40% reductions) subsequently reached maximum globularisation of 100% after 156 minutes and 400 minutes, respectively. Although the results of simulations suggest complete globularisation (i.e., 100%) for samples pre-forged to 20% reduction, the results of microstructure characterisations by SEM (Fig. 6c) confirmed that a small fraction of α-grains (i.e., < 5%) are yet to be globularised after FCTT. Despite the small level of uncertainty, the model simulation has been able to converge towards the experimental data efficiently.
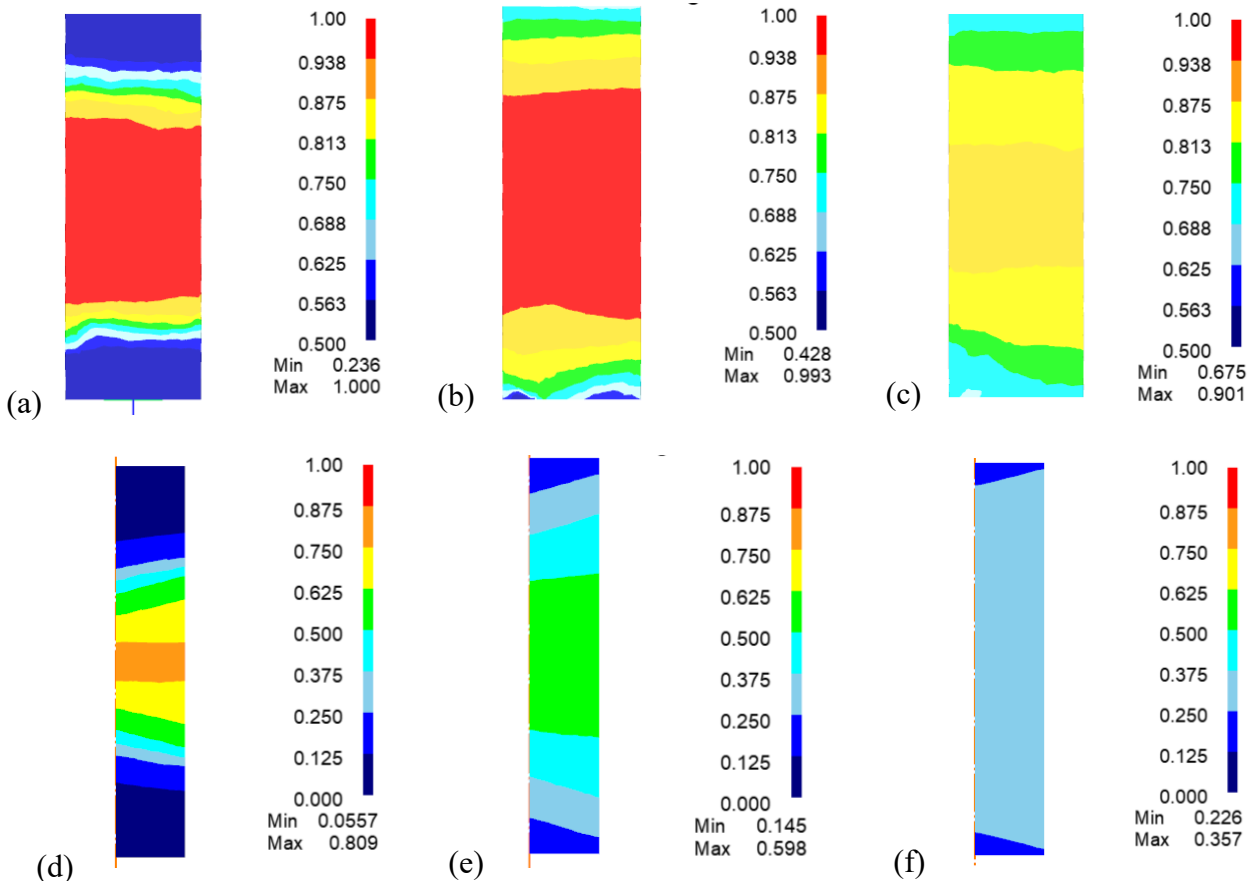
Figure 17: The results of predicted fraction of globularisation by FE simulation for FCTT after 9000 seconds, and at the end of ICTT . (a) & (d) samples forged to 60%, (b) & (e) samples forged to 40%, (c) & (f) samples forged to 20% in reduction, prior to CTT.

The results of FE simulations for the ICTT conditions revealed ~ 80%, %60 and 35% globularisation fractions for the sample conditions pre-forged to 60%, 40% and 20% reduction, respectively. The experimentally measured fractions of globularisation for these conditions were 86%, 54% and 28% respectively (Fig. 10a). The experimentally measured fractions of globularisation and the results of FE simulation were assessed on a 2D cross-section. The extent of globularisation within the samples subjected to CTT was varied depending on the level of applied strain during pre-CTT forging, and the method of cyclic treatment (i.e., ICTT or FCTT). The predicted results show variation in fraction of globularisation with strain, where a high degree of globularisation was obtained for the core of the sample which underwent high level of deformation (Fig. 17). The FE simuation of α-grain globularisation and growth were not extended to samples pre-forged at super-transus temperature of 1050 °C (i.e., β worked) due to the significant variations in the recrystallisaion mechanisms and the fact that the constitutive material model developed in this study is only valid for sub-transus conditions.

The comparative analyses of the predicted and measured fractions of globularisation after ICTT for the samples pre-forged at sub-transus temperature (i.e., 950 °C) revealed a good prediction accuracy with a maximum deviation of ~ 13% related to the sample forged to 20% reduction and subjected to ICTT (Fig. 18a). However, no data is provided in Fig. 18 for FCTT as the the FE simulations for FCTT resulted in complete globularisation of primary α-grains at the end of the cycle which were also confirmed by the experimental results, except for the sample pre-forged to 20% reduction for which 95% of α-grains was measured to be globulrsied (i.e., 5% uncertianity). Meanwhile, the predicted average grain size for all samples preforged at sub-transus temperature show a good agreement with the experimentally measured data after both ICTT and FCTT (Fig. 18 b). Nevertheless, the model successfully predicted the grain growth trend for both the FCTT and ICTT. The proposed model can further be enhanced by considering the physical significance of globularisation, dislocation density evolution and grain orientation relationships for varying microstructures.
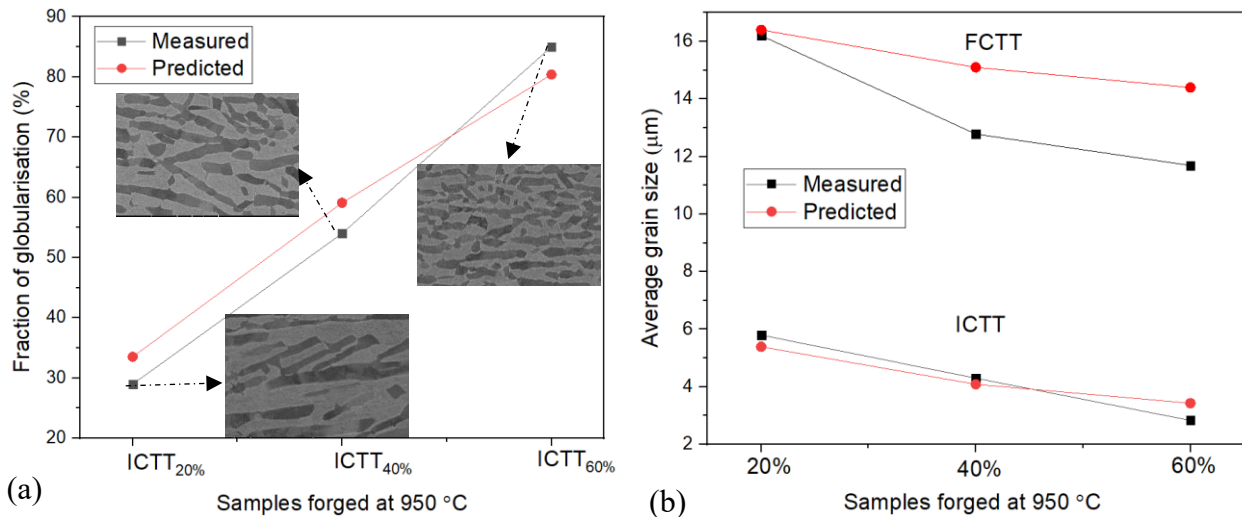
Figure 18: Comparison between the results of model prediction and experimentally measured data for (a) fraction of globularisation after ICTT, and (b) average grain size for the samples pre-forged to different levels of reduction at sub-transus temperature of 950 °C followed by FCTT and ICTT.

5.0 Conclusion

The present study explored the possibilities of microstructral modification in Ti-6Al-4V alloy by applying cyclic heat treatment with minimised sub-transus hot working. The main findings of these investigations are as follow:

- The samples forged at sub-transus temperature responded significantly to the cyclic thermal treatment (CTT) using both furnace (FCTT) and induction heating (ICTT). Meanwhile, the FCTT had resulted in maximum globularisation fraction compared to those subjected to ICTT.

- The low heating and cooling rates applied duirng the FCTT led to significant coarsening of α grains, whereas the ICTT resulted in the formation of fine α grains with a lower level of coarseing.

- The main globularisation mechanism was identified as the boundary splitting followed by thermal grooving for the samples pre-forged at sub-transus temperature regime. Whereas, a combination of edge spheroidisation and boundary splitting followed by thermal grooving was observed for the case of the samples pre-forged at teamperatures above β transus.

- A consititutive material model was developed, which was based on kinetic of globularisation and grain growth, and has effeciently been used to predict the extent of globularisation and grain size evolution for the different CTT trials examined.

- The material consititutive model was successfully incorporated into DEFORM® FE software package as a post-processing user subroutine to predict the evolution of globularisation and grain growth in primary α grains during forging and the subsequent cyclic heat treatments. The FE model was able to predict the trend and magnitudes of both globularisation and grain growth with small uncertainties, compared to the measured experimental data.

Acknowledgements

References

[1] M. Jackson, K. Dring, A review of advances in processing and metallurgy of titanium alloys, Mater. Sci. Tech., 22(8), (2013), 881-887.

[2] T. Seshacharyulu, S.C. Medeiros, J.T. Morgan, J.C. Malas, W.G. Frazier, Y.V.R.K. Prasad, Hot deformation and microstructural damage mechanisms in extra-low interstitial (ELI) grade Ti–6Al–4V, Mater. Sci. Engg.: A 279 (1–2), (2000), 289-299.

[3] S. Zherebtsov, M. Murzinova, G. Salishchev, S.L. Semiatin, Spheroidization of the lamellar microstructure in Ti–6Al–4V alloy during warm deformation and annealing, Acta Mater., 59(10), (2011), 4138-4150.

[4] N.S. Weston, M. Jackson, FAST-forge − A new cost-effective hybrid processing route for consolidating titanium powder into near net shape forged components, J Mater., Proces. Tech., 243, (2017), 335-346.

[5] D.J. Fray, Novel methods for the production of titanium, Int. Mater. Rev., 53(6), (2013), 317-325.

[6] R. Sabban, S. Bahl, K. Chatterjee, S. Suwas, Globularization using heat treatment in additively manufactured Ti-6Al-4V for high strength and toughness, Acta Mater., 162, (2019), 239-254.

[7] G.M. Ter Haar, T.H. Becker, Selective Laser Melting Produced Ti-6Al-4V: Post-Process Heat Treatments to Achieve Superior Tensile Properties, Mater., (Basel), 11(1), (2018).

[8] Z. Zhao, J. Chen, H. Tan, G. Zhang, X. Lin, W. Huang, Achieving superior ductility for laser solid formed extra low interstitial Ti-6Al-4V titanium alloy through equiaxial alpha microstructure, Scri. Mater., 146, (2018), 187-191.

[9] W. Szkliniarz, J. Chrapoński, A. Kościelna, B. Serek, Substructure of titanium alloys after cyclic heat treatment, Mater. Chem. Phy., 81(2-3), (2003), 538-541.

[10] P.M. Souza, P.D. Hodgson, B. Rolfe, R.P. Singh, H. Beladi, Effect of initial microstructure and beta phase evolution on dynamic recrystallization behaviour of Ti6Al4V alloy - An EBSD based investigation, J Alloy. Compd., 793, (2019), 467-479.

[11] X.G. Fan, H. Yang, S.L. Yan, P.F. Gao, J.H. Zhou, Mechanism and kinetics of static globularization in TA15 titanium alloy with transformed structure, J Alloy. Compd., 533, (2012), 1-8.

[12] J. Xu, W. Zeng, X. Zhang, D. Zhou, Analysis of globularization modeling and mechanisms of alpha/beta titanium alloy, J Alloy. Compd., 788, (2019), 110-117.

[13] L. da Silva, G. Sivaswamy, L. Sun, S. Rahimi, Effect of texture and mechanical anisotropy on flow behaviour in Ti–6Al–4V alloy under superplastic forming conditions, Mater. Sci.Engg.: A, 819, (2021).

[14] N. Stefansson, S.L. Semiatin, Mechanisms of globularization of Ti-6Al-4V during static heat treatment, Metal. Mater. Trans. A, 34(3), (2003), 691-698.

[15] H.K.a.O.I. H. Margolin and P. Cohen: in Titanium '80: Science and Technology, eds., TMS, Warrendale, PA, 1980, pp. 1555-61.

[16] E.B. Shell, S.L. Semiatin, Effect of initial microstructure on plastic flow and dynamic globularization during hot working of Ti-6Al-4V, Metal. Mater. Trans. A, 30(12), (1999), 3219-3229.

[17] W. Szkliniarz, G. Smołka, Analysis of volume effects of phase transformation in titanium alloys, J Mater. Proces. Tech., 53(1-2), (1995), 413-422.

[18] S. Roy, S. Suwas, Orientation dependent spheroidization response and macro-zone formation during sub β-transus processing of Ti-6Al-4V alloy, Acta. Mater., 134, (2017), 283-301.

[19] Y.C. Lin, M.-S. Chen, J. Zhong, Study of static recrystallization kinetics in a low alloy steel, Comput. Mater. Sci., 44(2), (2008), 316-321.

[20] N. Stefansson, S.L. Semiatin, D. Eylon, The kinetics of static globularization of Ti-6Al-4V, Metal. Mater. Trans. A, 33(11), (2002), 3527-3534.

[21] S. Roy, S. Karanth, S. Suwas, Microstructure and Texture Evolution During Sub-Transus Thermo-Mechanical Processing of Ti-6Al-4V-0.1B Alloy: Part II. Static Annealing in (α + β) Regime, Metal. Mater. Trans. A, 44(7), (2013), 3322-3336.

[22] S.L. Semiatin, J.C. Soper, I.M. Sukonnik, Grain growth in a conventional titanium alloy during rapid, continuous heat treatment, Scri. Metal. Mater., 30(7), (1994), 951-955.

[23] H. Hu, B.B. Rath, On the time exponent in isothermal grain growth, Metal. Trans., 1(11), (1970), 3181-3184.

[24] C.H. Johnson, S.K. Richter, C.H. Hamilton, J.J. Hoyt, Static grain growth in a microduplex Ti–6Al–4V alloy, Acta. Mater., 47(1), (1998), 23-29.

[25] E.A. Bel'skaya, E.Y. Kulyamina, Electrical resistivity of titanium in the temperature range from 290 to 1800 K, High. Temp., 45(6), (2007), 785-796.